Electron Capture Dissociation of Polypeptides using a 3 Tesla Fourier Transform Ion Cyclotron Resonance Mass Spectrometer

ARTICLE *in* RAPID COMMUNICATIONS IN MASS SPECTROMETRY · MAY 2002

Impact Factor: 2.25 · DOI: 10.1002/rcm.664 · Source: PubMed

4 AUTHORS, INCLUDING:

Nicolas Polfer
University of Florida
81 PUBLICATIONS **2,953** CITATIONS
SEE PROFILE

Kim Haselmann
Novo Nordisk
45 PUBLICATIONS **2,426** CITATIONS
SEE PROFILE

Roman Zubarev
Karolinska Institutet
251 PUBLICATIONS **10,892** CITATIONS
SEE PROFILE

RAPID COMMUNICATIONS IN MASS SPECTROMETRY
Rapid Commun. Mass Spectrom. 2002; **16**: 936–943
Published online in Wiley InterScience (www.interscience.wiley.com). DOI: 10.1002/rcm.664

RCM

Electron capture dissociation of polypeptides using a 3 Tesla Fourier transform ion cyclotron resonance mass spectrometer

Nicolas C. Polfer[1], Kim F. Haselmann[1], Roman A. Zubarev[2] and Pat R. R. Langridge-Smith[1]*

[1]Department of Chemistry, The University of Edinburgh, King's Buildings, West Main Road, Edinburgh EH9 3JJ, Scotland, UK
[2]Department of Chemistry, University of Southern Denmark, Campusvej 55, DK-5230 Odense M, Denmark

Received 7 March 2002; Accepted 7 March 2002

SPONSOR REFEREE: Kristina Håkansson, National High Magnetic Field Laboratory, Florida State University, 1800 East Paul Dirac Drive, Tallahassee, FL 32310, USA

Electron capture dissociation (ECD) of polypeptides has been demonstrated using a commercially available 3 Tesla Fourier transform ion cyclotron resonance (FTICR) instrument. A conventional rhenium filament, designed for high-energy electron impact ionisation, was used to effect ECD of substance P, bee venom melittin and bovine insulin, oxidised B chain. A retarding field analysis of the effective electron kinetic energy distribution entering the ICR cell suggests that one of the most important parameters governing ECD for this particular instrument is the need to employ low trapping plate voltages. This is shown to maximise the abundance of low-energy electrons. The demonstration of ECD at this relatively low magnetic field strength could offer the prospect of more routine ECD analysis for the wider research community, given the reduced cost of such magnets and (at least theoretically) the greater ease of electron/ion cloud overlap at lower field. Copyright © 2002 John Wiley & Sons, Ltd.

Electron capture dissociation (ECD)[1] has proven to be a valuable research tool for polypeptide sequencing and the localisation of post-translational modifications.[2–6] This fragmentation technique is complementary to the more established *heating* techniques, such as collisionally-activated dissociation (CAD)[7] and infrared multi-photon dissociation (IRMPD).[8] In combination with these other dissociation techniques, ECD can play an important role in *de novo* sequencing, where complete sequence coverage is required.

To date ECD has only been applied on Fourier transform ion cyclotron resonance mass spectrometers equipped with super-conducting magnets of 4.7 Tesla, or higher, field strength. The obvious advantages of higher field strength, B, are higher mass resolution (proportional to B) and the ability to trap more ions (proportional to B^2). However, at higher magnetic field, the ions and electrons are more tightly focused, potentially making their efficient overlap more difficult. The advantages of lower field magnets are reduced cost and greater magnetic field stability. The use of FTICR mass spectrometers equipped with lower field magnets could enable ECD mass spectra to be obtained more cost-effectively for lower mass compounds, such as tryptic digests of proteins, where high mass resolution is not as essential.

**Correspondence to*: P. R. R. Langridge-Smith, Department of Chemistry, The University of Edinburgh, King's Building, West Main Road, Edinburgh EH9 3JJ, Scotland, UK.
E-mail: prrls@ed.ac.uk

Since the electron capture cross-section increases with the charge squared (z^2) of the cationic species of interest, a requirement for ECD is an ionisation technique capable of generating multiply charged cations, such as electrospray ionisation (ESI). In order to increase the probability of electron capture, low-energy electrons (<0.2 eV) are also required.[1] This contrasts with the usual function of standard filament-based electron sources, which are designed for ionisation of neutral molecules by high-energy (e.g. 70 eV) electron impact.

A number of approaches have been proposed in order to improve ECD. McLafferty and co-workers[9] have used a design of ICR cell, consisting of an open-ended cylindrical cell with additional flat trapping plate electrodes, 'the nested ion cell geometry', which has enabled the simultaneous trapping of positively charged ions and electrons. They have reported ECD mass spectra for bovine ubiquitin showing extensive sequence coverage. However, the use of multiple electron irradiation (3 s) and storage (6 s) cycles (overall 10×9 s) increases the overall experimental time and can preclude the use of ECD in conjunction with on-line liquid chromatographic (LC) separation techniques.

In contrast, Tsybin *et al.*[10] and Haselmann *et al.*[11] have used indirectly heated high-surface area dispenser cathodes, in the former case fitted with a tungsten sponge impregnated with Ba-Ca aluminate, and in the latter a low work function BaO surface. Both groups have reported substantially reduced electron irradiation times, as short as 1 ms electron

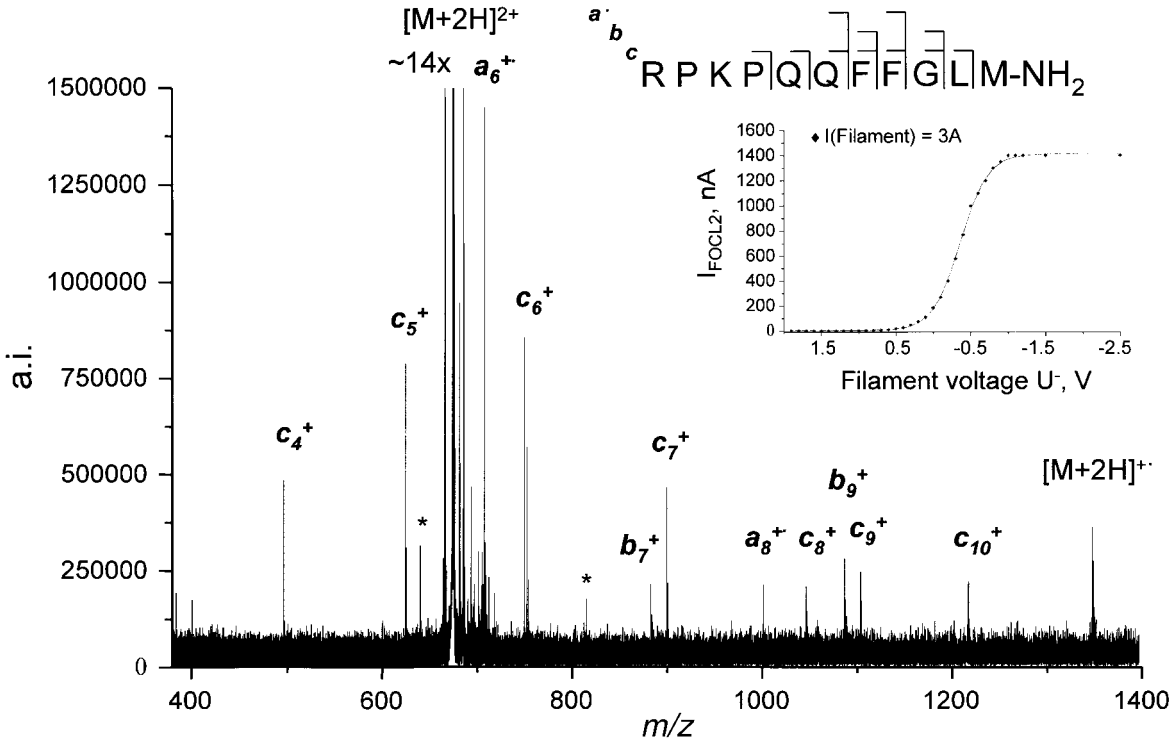

Figure 1. ECD mass spectrum of substance P in the 2+ charge state (40 scans). Electron irradiation time = 1 s. Asterisk denotes artefact peaks. The insert shows the electron current measured on the ion optic FOCL2, the rear element of the last Einzel lens that the ions pass through prior to entering the ICR cell, as a function of filament voltage U^-.

irradiation,[10,11] which are more compatible with those required for on-line LC.

The use of dispenser cathodes has been shown to markedly improve the rate of ECD. Primarily, this is due to the higher emission current and the larger emitting surface area, which result in emission of electrons with a larger beam diameter. This not only increases overlap of the electron beam with the ion cloud, but it has also been suggested[10] that the electron beam itself is large enough to confine the ion cloud, thereby creating a potential well that traps the ions in the radial direction in conjunction with the magnetic field. Nevertheless, these dispenser cathodes do present practical problems, such as increased blackbody radiation, which can lead to increased pressure within the ICR cell, as well as concerns regarding the possibility of contamination of the ICR cell with Ba sputtered from the cathode surface.

These different approaches to ECD have only been demonstrated by a select few research groups and are not generally available to the wider research community. Most commercially available FTICR instruments already are equipped with standard tungsten or rhenium filaments, which in principle should allow ECD to be performed. In this paper we report results on ECD experiments which were carried out on a commercial FTICR mass spectrometer (Bruker Daltonics APEX II) equipped with a 3 Tesla superconducting magnet and a standard rhenium filament as the electron source. Characterisation of the electron kinetic energy distribution from the rhenium filament was carried out in an attempt to optimise the efficiency of the ECD process.

EXPERIMENTAL

The polypeptides studied in this work were substance P (MW 1347.6), bee venom melittin (MW 2846.5), bovine insulin, oxidised B chain (MW 3495.9), and bovine ubiquitin (MW 8564.9), which were all obtained from Sigma and used without further purification. The compounds were dissolved in a water/methanol/acetic acid solution (49:49:2, v/v/v) to concentrations of between 10–100 μM. Electrospray ionisation (ESI) mass spectra were generated using an Analytica ion source (Branford, CT, USA), which is equipped with a standard glass capillary (end-caps metallised) and a storage hexapole. The solutions were infused using a syringe pump (Cole Parmer, IL, USA), at flow rates of between 80–120 μL/h. Mass spectra were recorded using a passively shielded 3 Tesla FTICR instrument (APEX II) manufactured by Bruker Daltonics (Billerica, MA, USA). The cations produced by ESI were accumulated for 500–1000 ms in the hexapole of the ion source before being injected into the Infinity™ ICR cell. The ions were trapped at low trapping plate voltages, typically 0.5 V, which were maintained during the entire experiment. No Sidekick™ or pulsed gas was used to assist trapping of the ions. Precursor ion isolation was achieved using a correlated sweep isolation of the most intense charge state. In the case of substance P, the doubly protonated precursor ion was isolated, whereas for both melittin and B chain insulin the quadruply protonated precursor ion was isolated. For ubiquitin no isolation was carried out. In order to induce ECD inside the ICR cell the cations were irradiated, for a

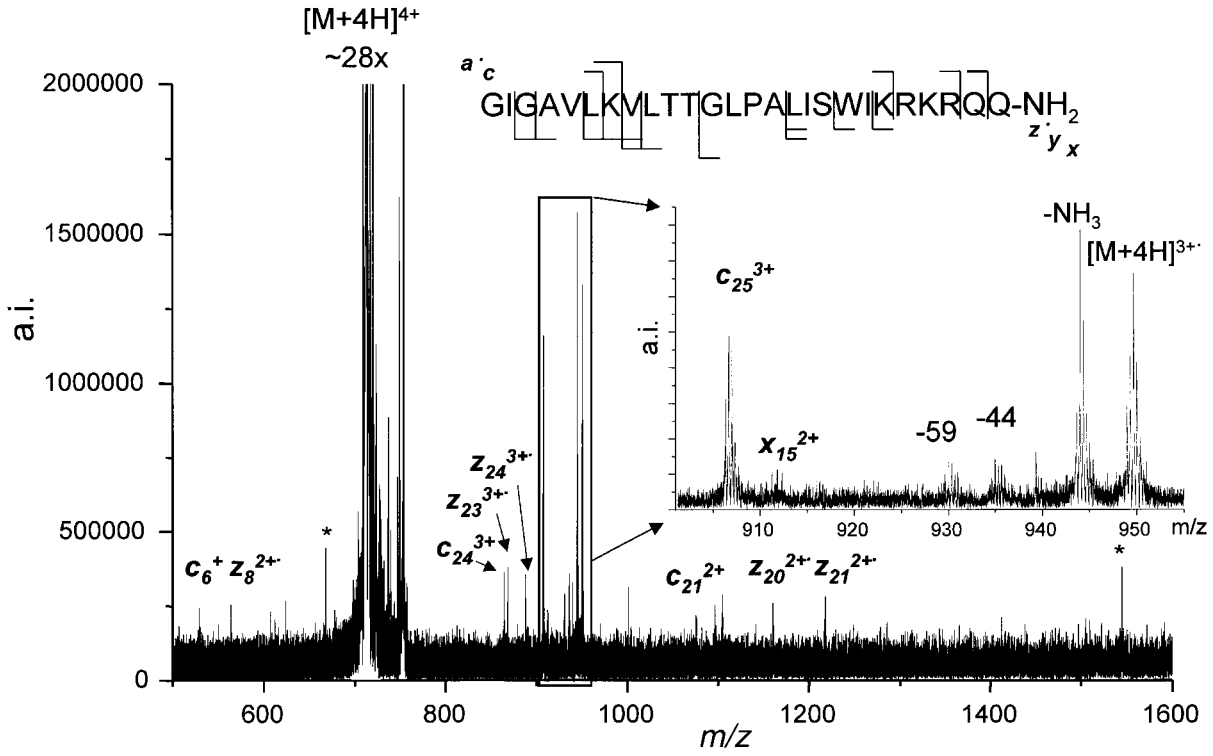

Figure 2. ECD mass spectrum of melittin in the 4+ charge state (100 scans). Electron irradiation time = 1.5 s. The insert shows an expansion of the *m/z* 950 region of the reduced species $[M + 4H]^{3+\cdot}$. Asterisk denotes artefact peaks.

period of 1–5 s, by low-energy electrons from a heated rhenium filament located 13 cm behind the ICR cell.

The rhenium filament (ca. 5 mm long Re ribbon, 0.038 × 0.51 mm, resistance 0.09959 Ohm/cm) was operated at a current of 3 A. During electron irradiation a voltage U^- (range −0.48 to +0.65 V) was applied to one side of the filament. As a consequence of the potential drop across the filament, a voltage U^+ ($U^+ = U^- + 2$ V) was measured on the other side of the filament. The emitted electron current was measured by using a picoammeter (model 610C; Keithley Instruments, Munich, Germany) at the Einzel lens element closest to the ICR cell (FOCL2). In the case of this particular instrument the filament voltage U^- at which no electron emission occurred was found to be +3.5 V. Detection of the precursor ions and their fragments was carried out in broadband mode using 512 K data points. No apodisation or extra zero-fill processing was carried out prior to fast Fourier transformation of the data. For all ECD mass spectra presented, between 40 and 200 scans were accumulated, unless otherwise stated.

RESULTS AND DISCUSSION

A prerequisite for ECD is good overlap of the ion cloud, trapped in the ICR cell, and the irradiating electron beam. The electron beam, however, has a small radius due to the effect of the magnetic field present and the limited surface area of the filament. For this design of ICR cell the trapping plates have small annular apertures (6 mm dia.). Trapping of ions on or very close to the centreline axis of the cell is therefore crucial. In order to trap ions at 0.5 V without Sidekick™ trapping or the use of a pulsed gas, the ion source and tuning parameters of the ion transfer optics had to be very carefully adjusted. The precursor ion magnitude had first to be maximised since electron irradiation was found to reduce the initial ion abundance by approximately two-thirds. Larger precursor ion magnitudes could be achieved by using higher trapping voltages. However, it was found that ECD was markedly reduced. The reason for this is discussed later.

The insert in Fig. 1 shows the current measured on the last Einzel lens element (FOCL2) that the ions pass through prior to entering the ICR cell, as a function of the filament voltage U^-. For experimentally favourable ECD conditions the optimum filament voltage U^- was found to be near +0.5 V; this corresponds to the onset of the steep rise in the emitted current. Another important parameter is the electron irradiation time. This must be long enough to permit sufficient electrons to enter the ICR cell, but not to lengthen excessively the acquisition time or to cause significant ion loss. Irradiation times of between 1 and 5 s were found to be sufficient. Since the ECD fragments are of low abundance the accumulation of several scans (S) is essential, thereby increasing the signal-to-noise (S/N) ratio by a factor of $\sqrt{S}$. This is a further reason for keeping the acquisition time for each single scan as short as possible. In the case of substance P, for example, 40 scans were found to be sufficient to generate ECD mass spectra with adequate sequence coverage.

ECD mass spectra

The ECD mass spectrum of the neuromodulator substance P

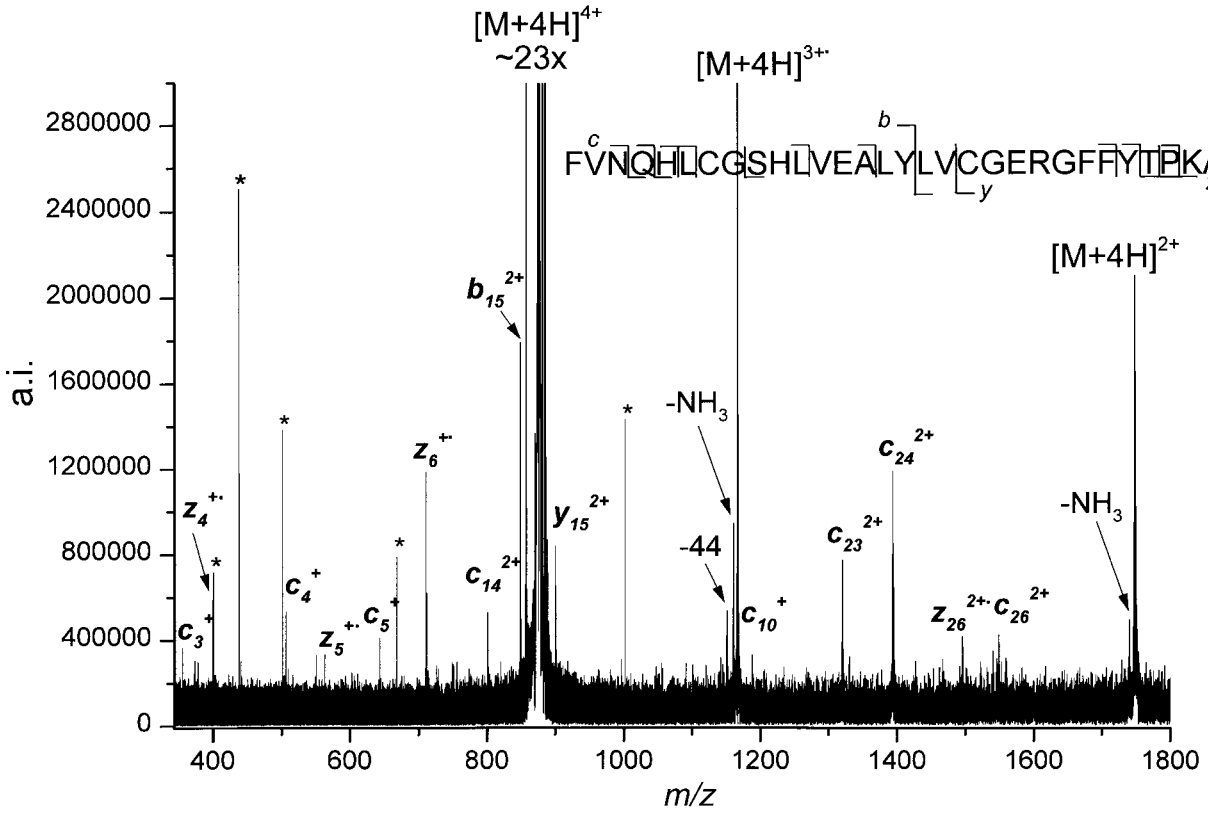

Figure 3. ECD mass spectrum of bovine insulin, oxidised B-chain, in the 4+ charge state (200 scans). Electron irradiation time = 5 s. Asterisk denotes artefact peaks.

is shown in Fig. 1. A 1-s electron irradiation time was used and 40 time-domain transients were accumulated. The N-terminal ***c***-ion fragments starting from c_4^+ to c_{10}^+ are visible in the mass spectrum. The c_8^+ fragment is of lowest abundance, with a S/N ratio of 10. This mass spectrum is representative of previously reported ECD mass spectra for this compound.[8] In the mass spectrum shown in Fig. 1, two ***b***-ions are present, suggesting that other activation mechanisms, as well as electron capture, took place. Vibrational excitation due to blackbody infrared irradiation from the heated filament could explain such fragment peaks. In addition, two odd electron ***a***-ions can also be seen in the mass spectrum.

For ECD of bee venom melittin, isolation of the quadruply protonated precursor ion was performed. The electron irradiation time was increased to 1.5 s. The optimum filament voltage U^-, where the reduced triply protonated species was just visible in a single scan, was found to be +0.65 V. The optimum filament voltage will probably vary from instrument to instrument, since the filament position, the ICR cell geometry and, most importantly the filament itself, will be different.

The ECD mass spectrum obtained for melittin is shown in Fig. 2. In this case, 100 scans were accumulated and a total of 17 ion fragments were observed, including four ***c***-ions, eight ***z***-ions, one ***a***-ions, three ***y***-ions and one ***x***-ion. Fragment peaks arising from the triply protonated reduced species ($[M + 4H]^{3+\cdot}$ at 949.59 Th) due to the typical small neutral losses expected in ECD, such as hydrogen desorption, ammonia and arginine side-chain losses, can also be seen. The mass resolution on the quadruply protonated precursor ion peak was approximately 18000. The individual peaks in the isotopic distribution had a symmetrical shape and were fully baseline resolved. For the reduced species the mass resolution dropped to 8000 and the peak shapes deteriorated slightly. Nevertheless, the mass resolving power of this 3 Tesla instrument was adequate since all the fragment peaks could be isotopically resolved.

In other experiments the 5+ charge state of melittin was isolated and subjected to ECD. However, no further structural information was gained. This was rather surprising, since the efficiency of electron capture increases with the square of the charge (z^2). The most likely explanation is due to the fact that the initial signal magnitude, after isolation, of the 5+ charge state of the precursor ion was only half that of the 4+ charge state. Addition of *m*-nitrobenzyl alcohol (*m*-NBA) was tried, in order to increase the signal magnitude at higher charge states,[9] but, although the relative abundance was shifted towards these higher charge states, the overall signal magnitude was suppressed.

SORI-CAD and IRMPD mass spectra were also recorded for the 4+ charge state of melittin. The typical ***b***- and ***y***-ion fragment pattern was observed (data not shown), which is complementary to the ECD fragmentation pattern. By combining the fragmentation data from the ECD mass spectrum as well as the SORI-CAD and IRMPD mass spectra, a total of 21 out of a possible 25 backbone bond cleavages could be identified.

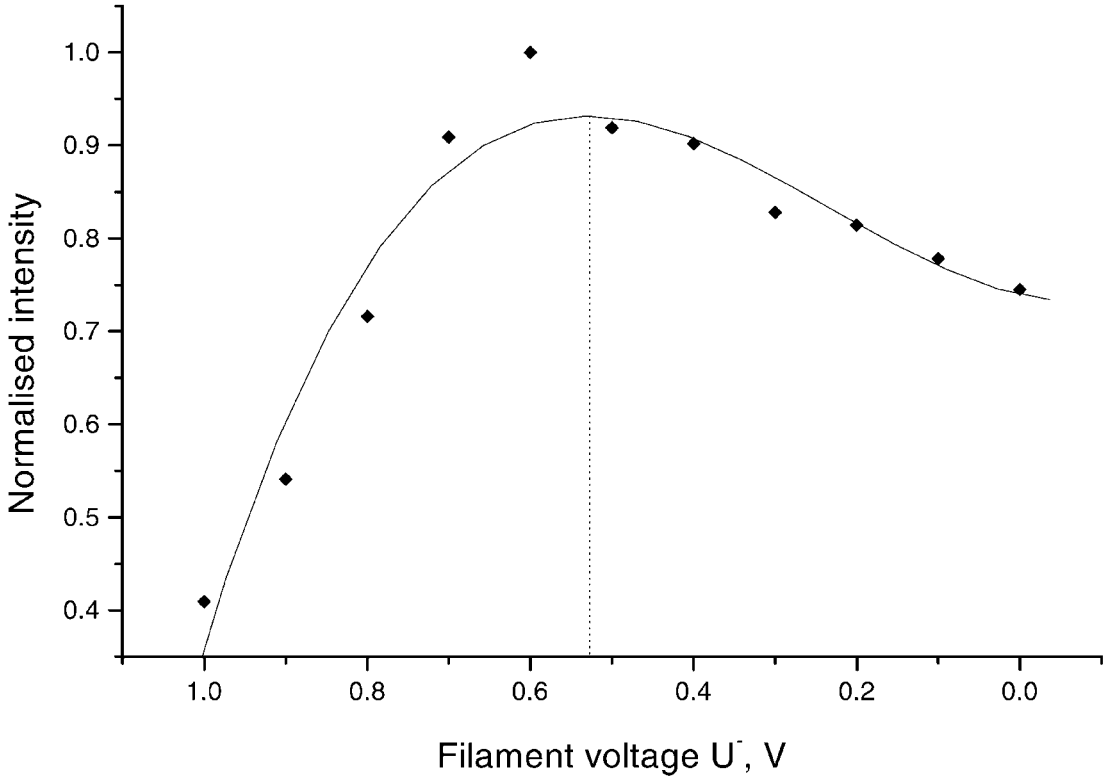

Figure 4. ECD fragment efficiency for substance P as a function of filament voltage U^-. The ECD fragment efficiency was calculated by adding the abundance of the ECD fragment peaks, c_4^+ to c_{10}^+, and normalising with respect to the mass spectrum with the highest ECD fragment efficiency.

The ECD mass spectrum for the 4+ charge state of bovine insulin, oxidised B chain, is shown in Fig. 3. This mass spectrum was generated by averaging 200 time-domain transients and employing a 5-s electron irradiation time. This translates into a total spectral accumulation time of slightly over 23 min, which is about 5 times longer than for melittin. The backbone bond cleavage was reduced to 13 out of a possible 29 bonds, equivalent to 45% sequence coverage. The B chain of insulin is modified by oxidation of the two cystein residues at position 7 and 19, resulting in an overall mass increase of 95.97 Da. However, no ambiguities were encounted in assigning the peaks nor did any loss of modification occur. In spite of the 5-s electron irradiation time employed, the mass resolution on the precursor ion peak was almost 40 000, indicating that the electron flux could be further increased without compromising the mass resolution or peak shapes.

Not surprisingly, the interresidue bond cleavage efficiency was observed to decrease, from substance P to bovine insulin, with increasing molecular weight due to the higher number of decomposition pathways and the larger degree of tertiary structure. Isolation of the 5+ charge state of bovine insulin, oxidised B-chain, was also attempted, but the signal magnitude was insufficient for assigning fragment ions.

To explore the limits of this 3 Tesla instrument, ECD was also attempted on bovine ubiquitin. In this case no mass isolation was carried out. The charge state distribution for this compound extended over the range 8+ to 13+. Despite averaging 200 time-domain transients, the resulting ECD mass spectrum only showed very limited fragmentation (data not shown). The reduced species, charge state 7+, was visible, as well as a number of fragment ions, including c_8^+, c_{24}^{3+}, c_{27}^{3+}, c_{31}^{4+}, z_{17}^{2+}, z_{17}^{3+}, z_{26}^{4+}, y_{18}^{2+}, y_{18}^{3+}, y_{24}^{4+} and b_3^+. Furthermore, peaks due the expected small neutral losses accompanying ECD were also seen in the mass spectrum. Whilst some degree of ECD seemed to have occurred, full interpretation of the mass spectrum is not possible due to insufficient mass resolving power to enable all of the fragment ions to be identified. Therefore, this size of peptide appears to be beyond the capability of this particular 3 Tesla FTICRMS instrument.

Characterisation of the rhenium filament

In order to gain a better understanding of the ECD process, measurements of the ECD fragment efficiency as well as the effective kinetic energy distribution of the electrons when entering the ICR cell as a function of the filament voltage U^- were carried out. The ECD efficiency was measured for substance P. The fragment efficiency was obtained by adding the abundance of the ECD fragment peaks c_4^+ to c_{10}^+ in each spectrum (of 40 scans). The data were then normalised with respect to the mass spectrum with highest fragment efficiency. The initial, non-fragmented, precursor ion magnitude was approximately the same in all spectra. Figure 4 shows the ECD fragment efficiency for the 2+ charge state of substance P as a function of the filament voltage U^-, confirming that maximum electron capture is observed at a filament voltage U^- just above +0.5 V. A third-

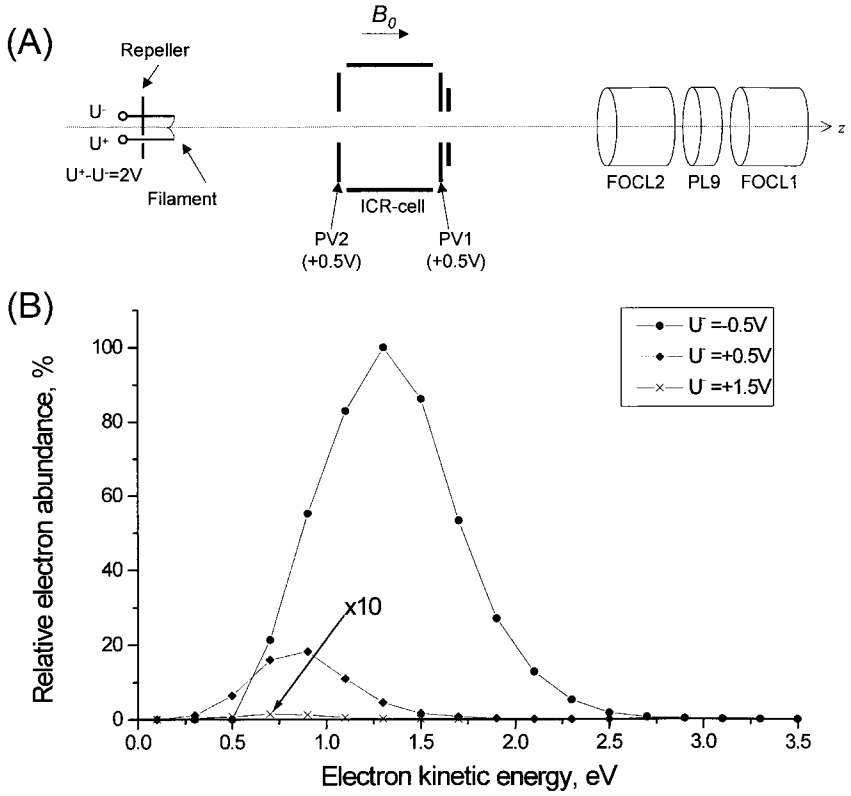

Figure 5. (A) Schematic diagram of the rhenium filament, ICR cell and the Einzel lens elements FOCL2, PL9 and FOCL1 on the APEX II instrument. The diagram is not drawn to scale. (B) The effective electron kinetic energy distribution at the rear trapping plate PV2 (held at +0.5 V during ECD experiments) for different filament voltages U^-. In the case of the distribution shown for a filament voltage $U^- = +1.5$ V, the y-axis intensity has been multiplied by a factor of 10 for clarity.

order polynomial expression was fitted to the data to estimate the voltage corresponding to maximum electron capture (+0.52 V). When the filament was turned on in advance and allowed sufficient time to reach operating temperature, this parameter (the voltage corresponding to maximum electron capture) was observed to be highly reproducible (±0.1 V). Furthermore, baking out the ICR cell with the filament on at regular intervals maintained the reproducibility.

The use of low trapping plate voltages (+0.5 V) on this particular instrument was observed to increase ECD. Conversely, increasing the voltage on the trapping plates gave rise to a reduction in ECD; for example, no ECD was observed at trapping plate voltages of 1 V. This could be due to a combination of factors, including higher on-axis velocities of both the ions and electrons, as well as increased magnetron motion of the ions. Another possible reason could be higher loss of electrons to the rear trapping plate (PV2), when more positive trapping plate voltages are applied. Experimentally, however, the emitted electron current measured on PV2 was found to be very low (<50 pA), indicating that the electron beam was tightly focused and that few electrons were lost to this trapping plate. Furthermore, when measuring the emission current at the Einzel lens element FOCL2, higher currents were observed at higher trapping plate voltages, suggesting higher extraction efficiency of the electrons.

One of the most important parameters for ECD is to employ low-energy electrons (<0.2 eV), which increases the electron capture cross-section. Since there is a potential energy difference between the filament, where the electrons are emitted, and the rear trapping plate,[14] this could be used as a means to alter the kinetic energy of the electrons entering the ICR cell in order to effect ECD.

Figure 5(A) shows a schematic diagram of the salient details of the APEX II instrument used in this work, showing the rhenium filament, ICR cell and the Einzel lens components FOCL2, PL9 and FOCL1. One side of the filament is held at a voltage U^- as well as the repeller plate. As a consequence of the potential drop across the filament, a voltage U^+ is measured on the other side of the filament, which is 2 V higher than U^-. The repeller plate is, therefore, negatively biased relative to U^+. Some of the emitted electrons travel in the z-direction (the same direction as the magnetic field B) through the ICR cell to the Einzel lens shown. The filament and the ICR cell are in the bore of the superconducting magnet, while the Einzel lens is situated outside the bore, in the fringing magnetic field. The magnetic field lines diverge substantially in the fringing field region, enabling the emitted electrons to be detected on the Einzel

lens. Experimentally, an electron current could only be measured on the element FOCL2 of the Einzel lens. An attempt was made to increase the number of electrons striking the element FOCL2 by employing a 'reverse' Sidekick™. However, this had no effect on the measured electron current. This would imply that most of the emitted electrons from the filament that passed through the ICR cell could be reliably detected at the element FOCL2.

Since it was the aim of this study to gain an understanding of the energetics of the electrons involved in ECD, only those electrons that passed through the ICR cell were of interest. Therefore, only the velocity component of the emitted electrons in the z-direction is of interest. While it is known that electrons are emitted in a range of angles from a thermionic electron emitter,[15] the resulting x- or y-velocity components of the electrons are likely to be small due to axialisation in the strong magnetic field. No attempt was made in this work to measure the actual emitted electron kinetic energy profile from the filament. Since ECD takes place in the ICR cell, it is only the kinetic energy distribution of the electrons entering the ICR cell that is of relevance for electron capture.

The effective kinetic energy distributions of the electrons entering the cell are shown in Fig. 5(B). These distributions were obtained by measuring the total electron current detected on the Einzel lens element FOCL2, which was held at ground potential, whilst varying the potential difference between the filament and the trapping plate PV2 (the trapping plate closest to the filament). This potential energy ramp provided a means of 'retarding field' analysis. For these measurements, the voltage on the trapping plate PV2 was initially set to a sufficiently negative value. At this voltage there was no transmission of emitted electrons through the ICR cell to the Einzel lens element FOCL2. The trapping plate voltage was then incrementally increased to 0 V, and then to positive values until there was no further increase in the measured electron current. For a filament voltage U^- of −0.5 V, a voltage of −2.4 V on the rear trapping plate PV2 was found to be just sufficient to retard the electrons sufficiently so that no current was observed. This implies that even the most energetic electrons had an effective kinetic energy at PV2 of 0 eV. When using a voltage of +0.5 V on the trapping plate PV2, as during an ECD experiment, such an electron would have an effective kinetic energy of 2.9 eV [0.5 −(−2.4)] when entering the ICR cell. The experimentally measured current profiles, I_{FOCL2} versus the retarding field voltage, were differentiated. The data from these differentiated current profiles was then plotted as a function of the effective kinetic energy of the electrons at PV2. This kinetic energy is the difference between the voltage applied to the rear trapping plate PV2 for the retarding analysis and the actual voltage applied to the trapping plate during an ECD experiment (+0.5 V). Figure 5(B) shows effective kinetic energy distributions for different values of U^-, and hence U^+.

As can be seen in Fig. 5(B), at a filament voltage U^- of −0.5 V the most abundant electrons have an effective kinetic energy of 1.3 eV and, at a filament voltage U^- of +0.5 V, the most abundant electrons have an effective kinetic energy of 0.9 eV. The effective kinetic energy of the most abundant electrons is higher when lower (i.e. more negative) filament voltages are used. Whilst the total emitted electron current is much larger at a filament voltage U^- of −0.5 V, compared to that at $U^- = +0.5$ V, the proportion of low-energy electrons is much greater for the kinetic energy distribution corresponding to a filament voltage of $U^- = +0.5$ V.

Currently, the abundance of the electrons in the low-energy tail of the kinetic energy distribution is not fully optimised. The only way to generate more low-energy electrons with the current approach is to reduce the trapping plate voltage, so that the kinetic energy of the electrons is effectively lowered since the retarding field is greater. Given that low trapping plate voltages were already employed (i.e. +0.5 V), there is not much scope left to further reducing the voltage on the trapping plates without compromising trapping of the ions.

CONCLUSIONS AND FUTURE WORK

It has been shown that a commercial 3 Tesla FTICR instrument (Bruker Daltonics APEX II) equipped with a conventional electron filament is capable of performing ECD on peptides with molecular weights up to 3.5 kDa. It has also been shown that in order to achieve ECD using this instrument one of the most important parameters is to employ low trapping plate voltages. The current electron source design, which is optimised for high-energy electron impact ionisation, limits the efficiency of ECD that can be achieved.

In future work the use of a modified filament design, incorporating a thorium coating, will be investigated. This should permit increased emitted electron flux from the filament at lower operating temperatures, which should decrease the achievable average electron kinetic energy. With this modified design it should be feasible, even on a 3 Tesla FTICR instrument, to generate sufficient ECD sequence information on peptides with molecular masses as high as 5 kDa. This would permit studies of post-translational modifications on most tryptic digest fragments, without the need to employ FTICR instruments equipped with larger, and more expensive, superconducting magnets.

Acknowledgements

The authors would like to thank Aventis Pharma (Dagenham, UK) for the donation of equipment, Dr. Don Daley (Argenta Discovery Ltd, Harlow, UK) for his support, and Professor Murray Campbell (The University of Edinburgh) for his helpful comments on the manuscript. N. Polfer would like to thank the Department of Chemistry (The University of Edinburgh) for the award of a Dewar-Ritchie Studentship.

REFERENCES

1. Zubarev RA, Kelleher NL, McLafferty FW. *J. Am. Chem. Soc.* 1998; **120**: 3265.
2. Kelleher NL, Zubarev RA, Bush K, Furie B, Furie BC, McLafferty FW, Walsh CT. *Anal. Chem.* 1999; **71**: 4250.
3. Mirgorodskaya E, Roepstorff P, Zubarev RA. *Anal. Chem.* 1999; **71**: 4431.
4. Stensballe A, Jensen ON, Olsen JV, Haselmann KF, Zubarev RA. *Rapid Commun. Mass Spectrom.* 2000; **14**: 1793.

5. Shi SD-H, Hemling ME, Carr SA, Horn DM, Lindh I, McLafferty FW. *Anal. Chem.* 2001; **73**: 19.
6. Håkansson K, Cooper HJ, Emmett MR, Costello CE, Marshall AG, Nilsson CL. *Anal Chem.* 2001; **73**: 4530.
7. Loo JA, Udseth HR, Smith RD. *Rapid Commun. Mass Spectrom.* 1988; **2**: 207.
8. Little DP, Speir JP, Senko MW, O'Conner PB, McLafferty FW. *Anal. Chem.* 1994; **66**: 2809.
9. Zubarev RA, Horn DM, Fridriksson EK, Kelleher NL, Kruger NA, Lewis MA, Carpenter BK, McLafferty FW. *Anal. Chem.* 2000; **72**: 563.
10. Tsybin YO, Håkansson P, Budnik BA, Haselmann KF, Kjeldsen F, Gorshkov M, Zubarev RA. *Rapid Commun. Mass Spectrom.* 2001; **15**: 1849.
11. Haselmann KF, Budnik BA, Olsen JV, Nielsen ML, Reis CA, Clausen H, Johnsen AH, Zubarev RA. *Anal. Chem.* 2001; **73**: 2998.
12. Axelsson J, Palmblad M, Håkansson K, Håkansson P. *Rapid Commun. Mass Spectrom.* 1999; **13**: 474.
13. Lavarone AT, Jurchen JC, Williams ER. *Anal. Chem.* 2001; **73**: 1455.
14. Håkansson K, Emmett MR, Hendrickson CL, Marshall AG. *Anal. Chem.* 2001; **73**: 3605.
15. Hutson AR. *Phys. Rev.* 1955; **98**: 889.